SIMS Microscopy Imaging of the Intratumor Biodistribution of Metaiodobenzylguanidine in the Human SK-N-SH Neuroblastoma Cell Line Xenografted into Nude Mice

J. Clerc, S. Halpern, C. Fourré, F. Omri, C. Briançon, J. Jeusset and P. Fragu

Equipe de Microscopie Ionique - INSERM U 66, Institut Gustave-Roussy, Villejuif Cedex, France

Microdosimetric evaluations of targeted radiotherapy of neuroblastoma with metaiodobenzylguanidine (MIBG) require precise assessment of the intracellular and intratumor distribution of the drug. We report the use of secondary ion mass spectrometry (SIMS) microscopy, a technique capable of mapping any chemical element within a biological specimen, to determine ^{127}I-MIBG biodistribution in human neuroblastoma SK-N-SH xenografted into nude mice. Highly specific images of ^{127}I-MIBG biodistribution were mapped within the tumor after in vivo administration of the drug and sample processing with cryotechniques (high-speed freezing and cryo-embedding), which prevent MIBG diffusion from original sites of uptake. We showed that the biodistribution of the tracer was highly nonuniform within the tumor. At the cellular level, most of the drug accumulated in the cytosol and perinuclear areas. In contrast, chemical sample processing provided not only a considerable loss in sensitivity due to passive diffusion of the drug in the organic solvents, but also artefactual images mainly due to MIBG redistribution onto the cell nuclei. Based on our findings in this SK-N-SH experimental tumor model, we suggest that MIBG should be attached to long-range emitters, in the hope of irradiating the many tumorous areas that remain carrier-free.

J Nucl Med 1993; 34:1565–1570

Due to its high sensitivity and specificity, radioiodine-labeled MIBG has been used successfully during the last decade to localize neuroblastoma and other neural crest tumors (*1,2*). Indeed, positive ^{123}I-MIBG scans can even be obtained in patients bearing neuroblastoma with very low uptake values of MIBG by the tumor (*3*). In contrast, targeted radiotherapy of neuroblastoma using ^{131}I-MIBG remains rather disappointing as only 30%–50% of patients will achieve some form of remission. Unfortunately, this is both incomplete and transitory in most cases. In addition, clinical outcome of the patients treated with MIBG is poorly correlated with values of the dose absorbed by the tumor and derived from gamma camera estimates of MIBG kinetics and uptake (*4*). This probably stems from the fact that the calculation of these values is based on the assumption that MIBG is homogenously distributed in the tumor. Precise determination of intracellular as well as intratumor drug localization is essential for a reliable microdosimetric evaluation of this targeted radiotherapy.

Although little is known about the intratumor pattern of MIBG biodistribution, its intracellular localization has already been achieved. In vitro experiments indicate that MIBG uptake is heterogeneous and that this tracer is almost totally located in the cytosol of neuroblastoma cells (*5,6*). However, its exact subcellular localization remains controversial since routine fixation procedures using organic solvents are unable to prevent the drug's diffusion from its original site of uptake (*7*).

To optimize MIBG therapy, the biodistribution of this tracer was determined both in its reference targeted tissue, the adrenomedulla, and in neuroblastoma xenografts into nude mice with the help of secondary ion mass spectrometry (SIMS) microscopy. This technique, developed in the early 1960s (*8*), provides images of distribution of many stable or radioactive nuclides, within biological tissues (*9*), has benefited from recent technological advances and may prove useful in solving certain biomedical problems (*10*). Special cryotechniques adapted to tissue sample processing and SIMS analysis requirements were applied in order to achieve in situ immobilization of ^{127}I-MIBG and subsequent ion microscope mapping representative of its in vivo biodistribution.

MATERIALS AND METHODS

Cells and Experimental Tumors

Two cell lines were tested for MIBG accumulation. The first was the SK-N-SH neuroblastoma cell line which has been previously described (*11*) and shown to actively take up MIBG in vitro (*12,13*). Cells were propagated in RPMI medium containing 12% fetal calf serum and penicillin/streptomycin (100 IU/ml) and trypsinized on average every five days. The second cell line was

Received Nov. 17, 1992; revision accepted May 25, 1993.

For correspondence or reprints contact: Dr. Jérôme Clerc, INSERM U 66, Laboratoire de Microscopie Ionique Analytique, Institut Gustave Roussy, 39 rue Camille Desmoulins, 94805 Villejuif Cedex, France.

the IGR-N-835 cell line, derived from a Stage IV abdominal neuroblastoma capable of secreting dopamine, which had been obtained from a 2-yr-old girl (*14*). To obtain experimental tumors, the flanks of 6- to 8-wk-old pre-irradiated (5 Gy) nude mice (SP Swiss) were inoculated either with 5×10^7 cells (SK-N-SH tumors) or with tumor fragments (IGR-N-835 tumors), obtained from a previously xenografted mouse. It took 8–10 wk to obtain SK-N-SH tumors measuring approximately 0.5 cm^3, while a shorter latency period (about 4 wk) was required for IGR-N-835 tumors.

Drugs

Iodine-127-MIBG (1300 μg/400 μl) was purchased from CIS Bioindustries Company (Gif-sur-Yvette, France). Iodine-125-MIBG (specific activity 1110 MBq/g) and ^{123}I-MIBG (specific activity 185 MBq/mg) used respectively for autoradiography or counting purposes were kindly donated by the same company. To determine whether in vivo MIBG accumulation was possibly cell-cycle dependent, we co-injected bromodeoxyuridine (BrdU, 100 μg/g, SIGMA Chemical, St. Louis, MO), a thymidine analog used as a proliferation marker (*15*). All drugs were injected intraperitoneally.

Protocols

MIBG Uptake by the Adrenals and Tumors. Iodine-123-MIBG uptake by the adrenals was first determined in 10 mice injected with about 1.85 MBq and results expressed as a percentage of the injected dose per gram of tissue (%ID/g). Likewise, MIBG uptake by tumors was determined both in mice bearing IGR-N-835 xenografts (n = 3) and SK-N-SH xenografts (n = 4). Mice were always killed for counting purposes 24 hr after administration of MIBG.

Microautoradiographies. Live animals (n = 2) were injected with about 185 MBq of ^{125}I-MIBG and killed 24 hr later. Tumors were cut in small fragments (n = 40) that first were transferred to plastic tubes containing 0.5 ml of fixative and counted. Adrenals were excised and counted in similar conditions. Chemical sample processing (see below) was carried out and semi-thin sections of the specimen were mounted on slides and coated with Amersham LM1 photographic emulsion. Exposure time was 10–30 days. Finally, preparations were stained with hematoxylin-eosin. In addition, loss of ^{125}I-MT/BG radioactivity by the fragments was systematically counted at each step of the chemical procedure.

SIMS Analysis. For SIMS experiments, ^{127}I-MIBG was administered intraperitoneally to the mice by escalating dose increments (0, 50, 200, 400 and 600 μg) and tumors were excised 24 hr later.

Fixative Procedures, Embedding and Sectioning. Both chemical and physical procedures were used for sample processing. With the chemical procedure, the tissue specimen was cut into 1–2 mm^3 fragments and fixed by immersion in a solution of 0.1% glutaraldehyde plus 2% paraformaldehyde in 0.1 *M* cacodylate buffer at a pH of 7.4. Fragments were then rinsed in the buffer, dehydrated in ethanol and embedded in methacrylate resin (Historesin, Pharmacia, Sweden). The physical procedure (cryotechnique) was used because MIBG has been reported to be a highly diffusible molecule, especially in organic solvents. With this method, tumors were cryofixed by ultra rapid immersion (5000 K sec^{-1}) in liquid propane, subcooled (77 K) by liquid nitrogen, cryosubstituted in acetone (183 K) and then embedded in Lowicryl K11M (Chemische Werke Lowi, Germany) at 213 K. Whatever the procedure, semi-thin sections (3 μm) were cut and laid on ultrapure gold holders at room temperature for SIMS analysis.

SIMS Microscopy: ^{127}I-MIBG Mapping. We used the IMS-3F microscope (CAMECA, Courbevoie, France) fitted with a digital imaging system designed to deal with specific biological problems, as previously described (*16,17*). A primary cesium ion beam (Cs^+) with an intensity of 10–25 nA and an energy of 10 KeV was focused on the surface (60 or 102 μm) of the resin-embedded specimen. Atoms situated in the superficial layers (1–5 nm) were progressively sputtered and possibly ionized. This technique is basically erosive and destroys the specimen while analyzing it. In routine working conditions, speed of erosion is about 1.5 nm per sec. Secondary ions, characteristic of the atomic composition of the analyzed area were then focused, energy filtered and separated by a mass spectrometer. The analytical ion images were finally displayed on a fluorescent screen coupled with a sensitive S.I.T video camera (LHESA SIT 4036). In a biological specimen, many ionized atoms are emitted as polyatomic cluster ions whose number of nucleons may be identical to that of the single ion of interest. Actual weight of these cluster ions is slightly different from that of the element to be mapped and can be eliminated by the mass spectrometer if a high mass resolution ($M/\Delta M > 2000$) is used. Unfortunately, working at high mass resolution reduces detection sensitivity. This drawback was attenuated by using high-speed integration for the elemental ion images, which improved the signal-to-noise ratio and optimized final image quality. In addition, local concentrations could be estimated by measuring intensity of the secondary ion beam of interest with an electron multiplier and using highly homogenous tissue equivalent standards (*18*).

Biodistribution of the drugs was delineated on detection of ^{127}I-MIBG and ^{81}Br (BrdU) while the histological structure of the specimen was visible through mapping of ^{31}P, which is especially abundant in the cell nuclei. The lateral resolution of the IMS-3F is 0.5 μm.

RESULTS

MIBG Uptake by Adrenals and Tumors

Mouse adrenals were found to have an ^{123}I-MIBG uptake of 2.3 ± 0.7 %ID/g at 24 hr. The IGR-N-835 tumors failed to accumulate MIBG. Values of uptake were ≤0.3 %ID/g which corresponded to "background" levels of nontarget tissue such as the liver or lungs. In contrast, with SK-N-SH xenografts, we found a value of 0.82 ± 0.30 %ID/g.

Iodine-125-MIBG Imaging of Tumors by Autoradiography

At the end of chemical processing, about 75% of the ^{125}I-MIBG activity was lost due to passive diffusion in the organic solvents. Images of MIBG biodistribution in the SK-N-SH xenografted tumors were obtained after 3–4 wk of exposure. A dramatically heterogeneous signal was obtained within the tumor. A few clusters of small round cells were intensely stained in the tumor. Positive staining was sometimes observed either in cells surrounding the vessels or in isolated large cells (Fig. 1). No significant ^{125}I-MIBG tissue binding was found in the slides obtained from IGR-N-835 xenografted tumors.

SIMS Mapping of ^{127}I-MIBG

Iodine-127-MIBG in the Adrenomedulla. A specific ^{127}I signal was observed in the adrenals of mice regardless of the level of MIBG administered (50–600 μg) with the chemical preparation. Drug biodistribution in the reference target organ involved the cytosol of the cells (Fig. 2), as previously reported (*19*).

Iodine-127-MIBG in the Tumors: Influence of Sample Preparation Technique. A specific SIMS signal of ^{127}I was always detectable for the 600-μg injected dose and ^{127}I-MIBG images of biodistribution could be visualized, regardless of the sample preparation procedures. Elemental mapping of ^{127}I revealed considerable heterogeneity of MIBG uptake among the cells and even more within the tumor. However, with the chemical processing procedure, large areas in tumor samples were found to be iodine-free.

At a dose of 400 μg, ^{127}I signal recovery was hardly ever constant in the analyzed areas of chemically prepared fragments. For this dose level, MIBG biodistribution was only displayed by SIMS in cell clusters capable of intense drug accumulation. Moreover, SIMS images of MIBG were observed both in the cytosol and on the nuclei of tumor cells with the chemical processing procedure (Fig. 3). In contrast, with cryo-prepared fragments, the ^{127}I signal was only emitted from the cytosol and perinuclear areas. Within the tumor, MIBG biodistribution was found to be highly nonuniform (Fig. 4). In addition, ^{127}I-MIBG could always be detected by processing high-resolution iodine spectra even when the secondary ion beam lacked sufficient intensity to provide reliable images corresponding to a reasonable depth range (500 nm) for SIMS analysis, which gradually destroys the specimen.

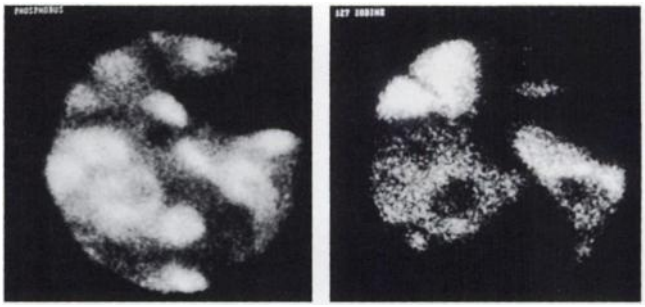

FIGURE 2. SIMS images of ^{127}I-MIBG within the adrenal medulla of mice after in vivo administration of the drug (400 μg) and chemical sample processing. Left view: The tissue structure is mapped through ^{31}P, which is especially abundant in cell nuclei. Right view: ^{127}I biodistribution showed cytosolic biodistribution of MIBG. Image fields: 60 μm.

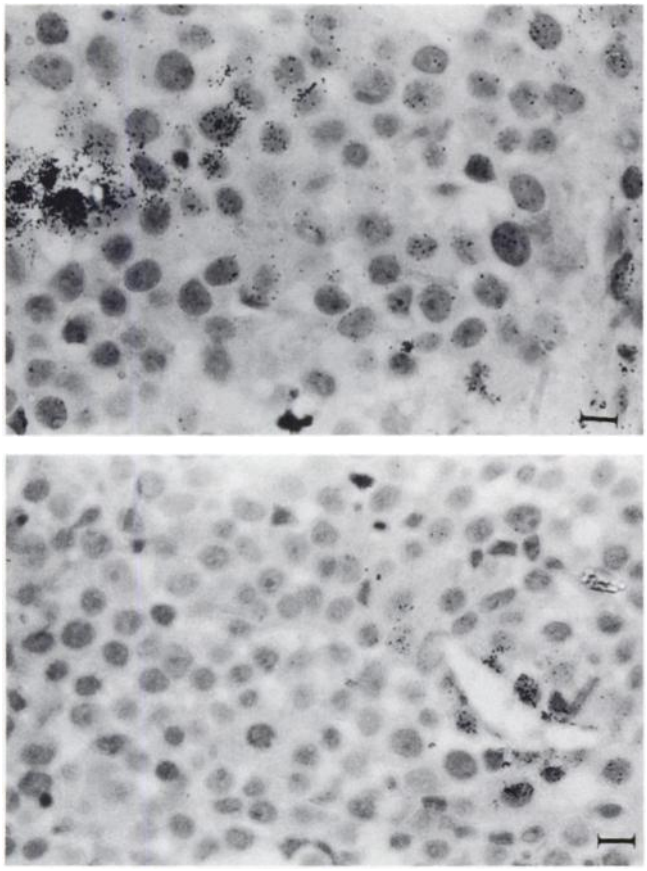

FIGURE 1. Autoradiographs of SK-N-SH neuroblastoma xenografted into nude mice injected (*ip*) with 1850 kBq of [^{125}I]-MIBG. Animals were killed 24 hr postinjection. Samples were exposed for 3 wk. Bar = 8 μm. Tumor biodistribution of MIBG was dramatically nonuniform (Top view). Sometimes, only perivascular (Bottom view) neuroblastoma cells were stained. Due to a chemical sample processing method that cannot prevent MIBG diffusion from original sites of uptake, no reliable information can be drawn regarding exact subcellular localization of the drug.

Based on comparison of ^{81}Br-BrdU and ^{127}I-MIBG biodistribution within the tumor, no clear-cut relationship could be found between tumor cell proliferation and a capacity for MIBG uptake in vivo. Indeed, although the most frequent feature encountered was either a simultaneous positivity or negativity for both ^{81}Br and ^{127}I, single staining could also be observed (Fig. 5).

DISCUSSION

The SIMS microscope IMS-3F proved to be effective in mapping ^{127}I-MIBG and its analytical capacity was sufficient to demonstrate a dramatically nonuniform pattern of MIBG biodistribution among tumor cells.

Choice of adequate model systems to study MIBG uptake is of paramount importance. Mechanisms of MIBG uptake have been extensively studied in the human neuroblastoma SK-N-SH cell line, in vitro (*7,12*). Two uptake systems are involved. The first one fulfills all the characteristics of the neuronal uptake-1 system (described for catecholamines), namely high specificity and affinity and saturability at extracellular concentration in the range of 10^{-6} *M*. This specific uptake-1 is mainly responsible for MIBG uptake in vivo and allows MIBG incorporation up to 30 times greater than the incorporation achieved by the second system which is likely to be simple diffusion (*13*). However, specific uptake depends on structural organization of the cells which conditions the number of cell contacts and on the preferential growth of certain cell subtypes, such as neuroblastic or Schwann-like cells, which coexist and may transdifferentiate (*5,20,21*). This prefer-

FIGURE 3. SIMS images of ^{127}I-MIBG in the SK-N-SH xenograft after in vivo administration of the drug (400 μg) and chemical sample processing. Tissue structure is delineated through ^{31}P (left view). Two cells had strongly incorporated bromodeoxyuridine, which is mapped through stable ^{81}Br (upper part of middle view). The ^{127}I distribution (right image) is exclusively in the few cells situated in the upper part of the image field. Due to inadequate use of a chemical sample processing, both images of uptake, in the cytosol, and of redistribution, onto the nuclei, are evidenced. Image fields: 102 μm.

ential growth probably occurs during xenografting and explains why most of these neuroblastoma cell lines partly (SK-N-SH) or totally (IGR-N-835) lose ability to take up MIBG, once inoculated in mice. Notwithstanding, higher values of uptake were found with the subcutaneous SK-N-SH tumor model when compared to those reported in MIBG positive human tumors (*3,22*). In addition, a variant of this tumor model has recently proved to be effective in studying ^{131}I-MIBG targeted radiotherapy (*23*). Xenografts are likely to mimic what actually occurs in human tumors because these models take into account drug accessibility to tumor cells. This may be critical for MIBG uptake by tumors since many positive cells were seen close to vessel lumens on the autoradiographs.

Sample processing techniques appeared to be crucial for assessing reliable images of MIBG biodistribution within biological materials. Indeed, drug diffusion in organic solvents is only limited in tissues that possess a specific intragranular storage system, such as the adrenals and pheochromocytoma. This corroborates the feasibility of MIBG detection by SIMS in the adrenals of mice even after injection of the lowest dose (50 μg) and chemical sample processing. Unfortunately, it is likely that MIBG storage in neuroblastoma is not dependent on the presence of specialized neurosecretory granules but only reflects a re-uptake mechanism of the drug (*24*). Thus, with chemical sample processing, most of the drug that had accumulated in the tumor was lost by diffusion in the solvents in such a way that the remaining staining only represented what had occurred in the cells exhibiting the highest MIBG uptake. Moreover, the intracellular localization of MIBG should be interpreted with great caution when using these methods, because we found that both uptake and redistribution images could be obtained.

Mapping of diffusible molecules such as MIBG in neuroblastoma must only be performed using cryoprepared

FIGURE 4. SIMS images of ^{127}I-MIBG in the SK-N-SH xenograft after in vivo administration of the drug (400 μg) and processing samples using high-speed freezing, cryo-substitution and cryo-embedding. Tissue structure was preserved and tumor nuclei were still mapped through ^{31}P (left view). Bromodeoxyuridine incorporated in the cells that underwent DNA synthesis (middle view). The ^{127}I-MIBG biodistribution appeared highly nonuniform in the tumor and involved the cytosol of the cells (right view). Image fields: 102 μm.

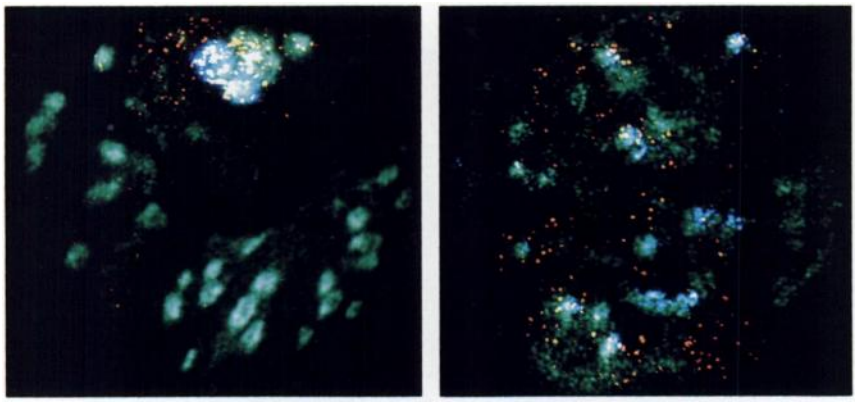

FIGURE 5. SIMS images of the superimposition of the elemental ion images corresponding to Figures 3 and 4, in pseudocolours. Tumor nuclei are imaged in green (^{31}P), 81 bromine of the BrdU in blue and ^{127}I of the MIBG in red to yellow. Using the chemical sample processing method (left view), MIBG was mapped both in the cytosol and artefactually onto cell nuclei (redistribution), while with the cryotechniques (right view), MIBG was only distributed in the cytosol. MIBG accumulation could be observed both in proliferative (BrdU positive) and nonproliferative cells (BrdU negative). Image fields: 102 μm.

tumor fragments (*25*). Unfortunately these methods are time consuming but were previously shown to be adapted to SIMS analysis of even high-speed diffusing elements such as calcium, potassium or sodium (*26*). Using the cryotechniques, we showed that the ^{127}I signal emanated mainly from the cytosol at the cellular level. However, minute traces of iodine distribution were, at times, evidenced at the periphery of cell nuclei, when superimposed with the image of nuclear phosphorus distribution (Fig. 5). This minor distribution may simply reflect the poor lateral resolution of the IMS-3F for imaging molecules situated close to the nucleus; this phenomenon may have been aggravated by the fact that many neuroblastoma cells had a small cytosol width (0.1–1 μm). However, the main reason this phenomenon occurred is that elemental ion images are acquired successively and represent deeper levels of analysis of the specimen, causing a further deterioration of the lateral resolution of up to 100–300 nm, especially when mapping trace elements for which longer analysis times (100–200 sec) are required.

Failure to obtain reliable ^{127}I-MIBG images in the SK-N-SH tumors for lower injected doses (50 and 200 μg), partly stemmed from the decision to work with high mass resolution ($M/\Delta M > 2000$), which undoubtedly affected amplitude of the specific signal (*27*). However, this was the only way to guarantee signal specificity, since a phosphorus cluster ion (126.980 uma) is always detected close to the iodine emission (126.907 uma). The detectable 400-μg injected dose of MIBG in the mice may have led to levels of concentration of the drug in the blood, for which both active and passive mechanisms of uptake could be involved. However, given that tumor uptake was bordering on 1 %ID/g, expected concentrations due to passive mechanisms of uptake would be below the threshold of detection of IMS-3F, which is of about 5 ppm (5 μg iodine per gram of tissue, assuming that the isotope is homogenously distributed in its matrix) (*18*). Mapping ^{127}I was achievable because it corresponded in positive cells to local concentrations of iodine in the range of detectability. Finally, we were unable to detect ^{127}I in the nontarget neuroblastoma IGR-N-835, even when larger doses of ^{127}I-MIBG (up to 800 μg/mouse) were injected although simple diffusion of the drug was bound to occur in the tumor. Given these reasons, it is clear that SIMS images of ^{127}I-MIBG in the SK-N-SH tumors mainly represent images of active uptake. However, the new generation of instruments that uses microprobes should further enhance detection sensitivity and provide subcellular scaled quantitative images (*10,28*).

Using innovative SIMS microscopy techniques, the present study addresses fundamental questions concerning optimization of metabolic radiotherapy with MIBG in experimental models. Our results on MIBG biodistribution in the SK-N-SH tumor model strongly suggest that MIBG should be attached to long-range particle emitters, in the hope of irradiating large tumor areas found to be more or less carrier-free by crossfire. Use of the ^{125}I to label MIBG (*29*) would be of limited interest, since its decay process results in a cascade of Auger electrons whose path range is too short for DNA targeting and because MIBG is localized in the cytosol. In addition, due to lack of uniformity in MIBG distribution within the tumor, ^{125}I labeling would lead to unchecked regions from which tumor regeneration could proceed (*30*).

In human beings, SIMS detection of tracers labeled with stable halogens, such as ^{127}I-MIBG, should be proposed for excised soft-tissue neuroblastoma, obtained after biopsy or surgery and previous administration of the "cold" drug. SIMS mapping of the tracer within the tumor would then provide a reliable biological model, which is a prerequisite for calculating the absorbed dose by computational Monte Carlo methods without neglecting intratumor heterogeneity of uptake. In addition, the amount of cold tracer injected would be identical to that used in therapy since we do not know whether use of test "hot" doses would reliably mimic the behavior of the therapeutic dose in MIBG therapy. Finally, the assessment of tissue specificity of new imaging or therapeutic agents, such as meta-bromobenzylguanidine, which can be labeled with the positron emitter ^{76}Br, are promising new directions for development of SIMS in improving nuclear imaging of neural crest tumors.

ACKNOWLEDGMENTS

The authors thank Dr. J. Benard (Laboratoire de Pharmacologie Clinique et Moléculaire, IGR) for providing the IGR-N-835

tumor; Dr. J. Lumbroso (Service de Médecine Nucléaire, IGR) for providing radiolabeled MIBG; Ms. L. Saint-Ange for editing the manuscript. This work was supported by a grant from the CNAMTS No. 998853.

REFERENCES

1. Lumbroso J, Guermazi J, Hartmann O, et al. Metaiodobenzylguanidine (MIBG) scans in neuroblastoma: sensitivity and specificity, a review of 115 scans. *Prog Clin Biol Res* 1988;271:689–705.
2. Hoefnagel CA, Voute PA, De Kraker J, Marcuse HR. Radionuclide diagnosis and therapy of neural crest tumors using iodine-131 metaiodobenzylguanidine. *J Nucl Med* 1987;28:308–314.
3. Moyes SE, Babich JW, Carter R, Meller ST, Agrawal M, McElwain TJ. Quantitative study of radioiodinated metaiodobenzylguanidine uptake in children with neuroblastoma: correlation with tumor histopathology. *J Nucl Med* 1989;30:474–480.
4. Hartmann O, Lumbroso J, Lemerle L, et al. The therapeutic use of iodine-131 metaiodobenzylguanidine (MIBG) in neuroblastoma: a phase II study in nine patients. *Med Pediatr Oncol* 1987;15:205–211.
5. Guerreau D, Thedrez Ph, Fritsch P, et al. In vitro therapeutic targeting of neuroblastoma using ^{125}I-labeled metaiodobenzylguanidine. *Int J Cancer* 1990;45:1164–1168.
6. Gaze MN, Huxham IM, Mairs RJ, Barrett A. Intracellular localization of metaiodobenzylguanidine in neuroblastoma cells by electron spectroscopic imaging. *Int J Cancer* 1991;47:875–880.
7. Smets LA, Janssen M, Rutgers M, Ritzen K, Buitenhuis C. Pharmacokinetics and intracellular distribution of the tumor-targeted radiopharmaceutical m-iodo-benzylguanidine in SK-N-SH neuroblastoma and PC-12 pheochromocytoma cells. *Int J Cancer* 1991;48:609–615.
8. Castaing R, Slodzian G. Microanalyse par émission ionique secondaire. *J Micros* 1962;1:395–414.
9. Galle P. Tissue localization of stable and radioactive nuclides by secondary-ion microscopy. *J Nucl Med* 1982;23:52–57.
10. Fragu Ph, Briançon C, Fourré C, et al. SIMS microscopy in the biomedical field. *Biol Cell* 1992;74:5–18.
11. Biedler JL, Helson L, Spengler B. Morphology and growth, tumorigenicity, and cytogenesis of human neuroblastoma cells in continuous culture. *Cancer Res* 1973;33:2643–2652.
12. Buck J, Bruchelt G, Girgert R, Treuner J, Niethammer D. Specific uptake of m-[^{125}I]Iodobenzylguanidine in the human neuroblastoma cell line SK-N-SH. *Cancer Res* 1985;45:6366–6370.
13. Smets LA, Loesberg C, Janssen M, Metwally EA, Huiskamp R. Active uptake and extravesicular storage of m-Iodobenzylguanidine in human neuroblastoma SK-N-SH cells. *Cancer Res* 1989;49:2941–2944.
14. Bettan-Renaud L, Bayle Ch, Teyssier JR, Benard J. Stability of phenotypic and genotypic traits during the establishments of a human neuroblastoma cell line, IGR-N-835. *Int J Cancer* 1989;44:460–466.
15. Van Oostrum IEA, Rozemuler E, Kuol RFG, Erkens-Schulze S, Rutgers DH. Cell proliferation kinetics of six xenografted human cervix carcinomas: comparison of autoradiography and bromodeoxyuridine labelling methods. *Cell Tissue Kinet* 1990;23:523–544.
16. Olivo JC, Khan E, Halpern S, Briançon C, Fragu P, Di Paola R. Microcomputer system for ion microscopy digital imaging and processing. *J Microscopy* 1989;56:105–114.
17. Fourré C, Halpern S, Jeusset J, Clerc J, Fragu Ph. Significance of SIMS microscopy for Technetium-99m mapping in leucocytes. *J Nucl Med* 1992; 33:2162–2166.
18. Jeusset J, Halpern S, Briançon C, Garcia F, Fragu Ph. Halogens standardization by SIMS microscopy for applications in biological samples [Abstract]. *Biol Cell* 1992;75:8a.
19. Telenczak P, Ricard M, Halpern S, Fragu P. A method to evaluate the tissue absorbed dose in metabolic radiotherapy: preliminary results with mIBG. In: Benninghoven A, Evans C, McKeegan K, Storms H, Xerner H, eds. *Secondary ion mass spectrometry, SIMS VII* Chichester: Wiley and Sons, 1988:315–318.
20. Biedler JL, Spengler BA, Chang TD, Ross R. Transdifferentiation of human neuroblastoma cells results in coordinate loss of neuronal and malignant properties. In: Evans AE, D'Angio GJ, Seeger RC, eds. *Advances in neuroblastoma research 2*. New York: Wiley-Liss; 1988:265–276.
21. Trojanowski JQ, Molenaar WM, Baker DL, Pleasure D, Lee VM. Neural and neuroendocrine phenotype of neuroblastomas, ganglioneuroblastomas, ganglioneuromas and mature versus embryonic human adrenal medullary cells. In: Evans AE, D'Angio GJ, Seeger RC, eds. *Advances in neuroblastoma research 3*. New York: Wiley-Liss; 1991:335–341.
22. Kemshead JT, Pizer BL, Patel K. In: Pochedly C, ed. *Neuroblastoma: tumor biology and therapy. neuroblastoma: perspective for future research*. Boca Raton: CRC Press, 1990:383–385.
23. Rutgers M, Gubbels AAT, Hoefnagel CA, Voûte PA, Smets LA. A human neuroblastoma xenograft model for [^{131}I]-metaiodobenzylguanidine (MIBG) biodistribution and targeted radiotherapy. In: Evans AE, D'Angio GJ, Seeger RC, eds. *Advances in neuroblastoma research 3*. New York: Wiley-Liss; 1991:471–478.
24. Montaldo PG, Lanciotti M, Casaralo A, Cornaglia-Ferraris P, Ponzoni M. Accumulation of m-iodobenzylguanidine by neuroblastoma cells results from independent uptake and storage mechanisms. *Cancer Res* 1991;51: 4342–4346.
25. Kellenberg E. The potential of cryofixation and freeze substitution: observations and theoritical considerations. *J Microsc* 1991;161:183–203.
26. Stelly N, Halpern S, Nicolas G, Fragu P, Adoutte A. Ion imaging in cryofixed paramecium: high Ca^{2+} concentration in the cortex [Abstract]. *Biol Cell* 1990;69:20a.
27. Halpern S, Fragu P, Briançon C, Larras-Regard E. Contribution of the high mass resolution in trace element imaging in biology. In: Benninghoven A, Evans C, McKeegan K, Storms H, Xerner H, eds. *Secondary ion mass spectrometry SIMS VI*. Chichester: Wiley and Sons; 1987:897–900.
28. Slodzian G, Daigne B, Girard F, Boust F, Hillion F. Scanning secondary ion analytical microscopy with parallel detection. *Biol Cell* 1992;74:43–50.
29. Sisson JC, Hutchinson RJ, Shapiro B, et al. Iodine-125-MIBG to treat neuroblastoma: preliminary report. *J Nucl Med* 1990;31:1479–1485.
30. O'Donoghue JA, Wheldon TE, Babich JW, Moyes SE, Barett A, Meller ST. Implications of the uptake of ^{131}I-radiolabeled metaiodobenzylguanidine (MIBG) for the targeted radiotherapy of neuroblastoma. *Br J Radiol* 1991;64:428–434.